THE JOURNAL OF BIOLOGICAL CHEMISTRY VOL. 291, NO. 23, pp. 11993–12002, June 3, 2016

Reduction of Flavodoxin by Electron Bifurcation and Sodium Ion-dependent Reoxidation by NAD^+ Catalyzed by Ferredoxin-NAD^+ Reductase (Rnf)*

Received for publication, March 8, 2016, and in revised form, April 1, 2016 Published, JBC Papers in Press, April 5, 2016, DOI 10.1074/jbc.M116.726299

Nilanjan Pal Chowdhury[‡§], Katharina Klomann[‡], Andreas Seubert[¶], and Wolfgang Buckel[‡§1]

From the [‡]Laboratorium für Mikrobiologie, Fachbereich Biologie and Synmikro and the [¶]Fachbereich Chemie, Philipps-Universität, 35032 Marburg, and the [§]Max-Plank-Institut für terrestrische Mikrobiologie, 35043 Marburg, Germany

Electron-transferring flavoprotein (Etf) and butyryl-CoA dehydrogenase (Bcd) from *Acidaminococcus fermentans* catalyze the endergonic reduction of ferredoxin by NADH, which is also driven by the concomitant reduction of crotonyl-CoA by NADH, a process called electron bifurcation. Here we show that recombinant flavodoxin from *A. fermentans* produced in *Escherichia coli* can replace ferredoxin with almost equal efficiency. After complete reduction of the yellow quinone to the blue semiquinone, a second 1.4 times faster electron transfer affords the colorless hydroquinone. Mediated by a hydrogenase, protons reoxidize the fully reduced flavodoxin or ferredoxin to the semi-reduced species. In this hydrogen-generating system, both electron carriers act catalytically with apparent K_m = 0.26 μM ferredoxin or 0.42 μM flavodoxin. Membrane preparations of *A. fermentans* contain a highly active ferredoxin/flavodoxin-NAD^+ reductase (Rnf) that catalyzes the irreversible reduction of flavodoxin by NADH to the blue semiquinone. Using flavodoxin hydroquinone or reduced ferredoxin obtained by electron bifurcation, Rnf can be measured in the forward direction, whereby one NADH is recycled, resulting in the simple equation: crotonyl-CoA + NADH + H^+ = butyryl-CoA + NAD^+ with K_m = 1.4 μM ferredoxin or 2.0 μM flavodoxin. This reaction requires Na^+ (K_m = 0.12 mM) or Li^+ (K_m = 0.25 mM) for activity, indicating that Rnf acts as a Na^+ pump. The redox potential of the quinone/semiquinone couple of flavodoxin (Fld) is much higher than that of the semiquinone/hydroquinone couple. With free riboflavin, the opposite is the case. Based on this behavior, we refine our previous mechanism of electron bifurcation.

The fermentation of sugars and amino acids to butyrate is a characteristic feature of anaerobic bacteria of the Firmicutes phylum. In the human gut, butyrate is derived from the microbial degradation of fibers, *i.e.* oligosaccharides or peptides that are non-digestible by human enzymes (1, 2). Butyrate nourishes the epithelia cells of the gut and thus is essential for human health (3, 4). Until recently, the production of butyrate by bacteria was regarded as a mere disposal for reducing equivalents. In 2008, however, it was established that the butyrate-forming pathway contributes to hydrogen formation and energy conservation, because the exergonic reduction of crotonyl-CoA to butyryl-CoA by NADH is also tightly coupled to the endergonic reduction of ferredoxin (Fd^-)[2] by NADH. This process has been called electron bifurcation, because the two electrons supplied by NADH ($E^{\circ\prime}$ = −320 mV) move to different potentials: one electron goes to the high potential crotonyl-CoA ($E^{\circ\prime}$ = −10 mV), and the other goes to the low potential ferredoxin ($E^{\circ\prime}$ = −405 mV; E' ≤ −500 mV). Repetition of this process affords butyryl-CoA and two reduced ferredoxins (Fd^{2-}) (5–7). This "energy-rich" electron carrier gives rise to molecular hydrogen and/or recycles NADH mediated by a ferredoxin-NAD^+ reductase also called ferredoxin/flavodoxin-NAD reductase (Rnf) (8, 9). The energy difference between reduced ferredoxin and NAD^+ of about 200 mV is proposed to be used by this integral membrane enzyme to generate an electrochemical H^+ or Na^+ gradient. In *Acidaminococcus fermentans* (10) and *Megasphaera elsdenii* (11), both of which belong to the Negativicutes of the Clostridia (12), the electron-bifurcating reduction of crotonyl-CoA is catalyzed by two enzymes. One is a heterodimeric electron-transferring flavoprotein (EtfAB), which contains one FAD on each subunit (α and β-FAD on subunit A and B, respectively), and the other is a homotetrameric butyryl-CoA dehydrogenase (Bcd) with one FAD (δ-FAD) on each subunit. Based on protein crystallography and enzymatic assays, we propose that NADH reduces β-FAD to the hydroquinone (β-$FADH^-$), which delivers one electron further to the high potential α-FAD that is 14 Å apart to become a stable anionic semiquinone (α-$FAD^{\bullet-}$). The remaining low potential and highly reactive β-$FADH^\bullet$ donates its electron further to ferredoxin. Then α-$FAD^{\bullet-}$, located on a flexible domain, swings to the FAD of Bcd (δ-FAD) and transfers its electron to yield δ-$FADH^\bullet$. Finally, the second round generates δ-$FADH^-$, which reduces crotonyl-CoA to butyryl-CoA (10, 11).

It has been known for a long time that under iron-limiting conditions, flavodoxin (Fld) replaces ferredoxin (13). One well studied organism in this respect is *A. fermentans*, which grows at equal rates either at 7 μM or at 45 μM Fe^{2+} in the medium. At 7 μM Fe^{2+}, the cells contain 3.5 μmol flavodoxin g^{-1} of protein (1.4 mM) but only 0.02 μmol ferredoxin g^{-1} of protein, whereas

* This work was supported in part by a grant from the German Research Foundation (DFG). The authors declare that they have no conflicts of interest with the contents of this article.

[1] To whom correspondence should be addressed: Laboratorium für Mikrobiologie, Fachbereich Biologie, Karl-von-Frisch-Str. 8, 35032 Marburg. Tel.: 49-6421-28-22088; Fax: 49-6421-28-28979; E-mail: buckel@staff.uni-marburg.de.

[2] The abbreviations used are: Fd, ferredoxin; Etf, electron-transferring flavoprotein; Bcd, butyryl-CoA dehydrogenase; Fld, flavodoxin; Rnf, ferredoxin-NAD reductase; Rf, riboflavin; ICP-MS, inductively coupled plasma mass spectrometry; MPa, megapascals.

at 45 μM Fe^{2+}, the flavodoxin content decreases to 0.2 μmol g^{-1} and that of ferredoxin increases to 1.0 ± 0.1 μmol g^{-1} of protein (0.4 mM) (14). Flavodoxin from *A. fermentans* is a protein (molecular mass = 14.5 kDa) with FMN as tightly bound cofactor. Ferredoxin from the same organism is a smaller protein (molecular mass = 5.6 kDa) that contains two [4Fe-4S] clusters. The redox potentials of both electron carriers from *A. fermentans* have been measured. In the case of ferredoxin, the first electron encounters a potential of $E_1{}^{\circ\prime} = -340$ mV (Fd/Fd^-), and the second electron encounters a potential of $E_2{}^{\circ\prime} = -405$ mV (Fd^-/Fd^{2-}) (14); with flavodoxin, the corresponding potentials are $E_1{}^{\circ\prime} = -60$ mV and $E_2{}^{\circ\prime} = -430$ mV (15). Hence, from a thermodynamic point of view, flavodoxin can easily replace ferredoxin, if only the half/fully reduced carriers with the low redox potentials ($E_2{}^{\circ\prime}$) are involved. In a previous study, evidence was obtained that ferredoxin cycles between half/fully reduced states (Fd^-/Fd^{2-}) during electron transfer from Etf to hydrogenase and back (10). This study will show that flavodoxin behaves in a similar manner; it cycles between the neutral blue semiquinone ($FldH^{\bullet}$) and the colorless hydroquinone ($FldH^-$) states, which are much easier to detect than the brownish/colorless $Fd/Fd^-/Fd^{2-}$ states. Furthermore, the generation of two-electron reduced ferredoxin and flavodoxin by electron bifurcation without the use of artificial electron donors allowed the confirmation of the postulated Na^+ dependence of the Rnf from *A. fermentans*.

Materials and Methods

Growth of Microorganisms—*A. fermentans* strain VR4 (DSM 20731) was grown anaerobically on the glutamate/yeast extract/biotin medium as described earlier (16). *Clostridium tetanomorphum* DSM 526 was grown on the same glutamate medium but without added biotin. *Clostridium pasteurianum* DSM 525 was grown on a medium containing 100 mM glucose, 70 mM $NaHCO_3$, and yeast extract (2 g/liter). *E. coli* strains DH5α and BL21-DE3 were grown aerobically at 37 °C in Standard I nutrient broth (Merck, Darmstadt, Germany) using an orbital shaker. For growth of *E. coli* with inserted plasmids, the medium was supplemented with carbenicillin (50 μg/ml). For overproduction of flavodoxin, 2 liters of Standard I broth, supplemented with carbenicillin, was inoculated with 25 ml of an overnight culture of BL21-DE3 that has been transformed with the pASG-IBA33 expression vector (IBA, Göttingen, Germany) containing the flavodoxin gene of *A. fermentans*. The culture was grown until it reached $OD_{600} = 0.6$, and then anhydrotetracycline (200 μg/liter, IBA) was added to induce the expression of the recombinant gene during the further growth for the next 12 h at room temperature. The harvested cell paste was stored at −80 °C until use.

Synthesis of CoA Esters—Crotonyl-CoA and butyryl-CoA were synthesized by acylation of CoASH in aqueous 1 M $KHCO_3$ using 1 M crotonic anhydride or butyric anhydride in acetonitrile with a slight molar excess. After acidification, the CoA thioesters were purified over C18 columns and stored as lyophilized powders at −80 °C (17). The concentration of crotonyl-CoA was calibrated by the NAD^+-dependent β-oxidation to acetyl-CoA and acetyl phosphate as described for the assay of glutaconyl-CoA decarboxylase (16). HPLC of crotonyl-CoA and butyryl-CoA was performed on a C18 Kinetex column (5-μm particle size, 100-Å pore size, 250 × 4.6 mm, Phenomenex, Aschaffenburg, Germany) at a flow rate of 1 ml/min in 50 mM KH_2PO_4, pH 5.3, and 5% acetonitrile. During 20 min, a linear gradient up to 60% acetonitrile was applied. For detection of respective CoA esters from the assay mixtures, samples were acidified with concentrated HCl to pH 2.0, centrifuged, and filtered to remove the denatured protein. Samples of 10 μl were loaded on the HPLC column.

Preparation of Ti(III) Citrate—Ti(III) citrate was prepared as described (18). $TiCl_3$ in HCl (12%, 0.5 ml) was added to 5 ml of 0.2 M sodium citrate. After 10 min, the mixture was neutralized with a saturated sodium carbonate solution to pH 7.0. The prepared Ti(III) citrate was stored under anaerobic conditions in air-tight bottles.

Recombinant DNA Methods—Genomic DNA was isolated from *A. fermentans* cells using a genomic DNA preparation kit (Fermentas, Thermo Fisher) according to the manufacturer's instructions. The flavodoxin protein from *A. fermentans* was identified earlier by N-terminal sequencing (15). The gene corresponding to the protein, *Acfer_0269* (19), was amplified by PCR using genomic DNA as the template with the forward primer 5′-AAGCTCTTCAATGAGCAAAATCGCAGTGGTGTTCT and the reverse primer 5′-AAGCTCTTCACCCTGCCAGCGCCTCTCCCAG. The PCR product was cloned into the p-ENTRY vector and introduced in *E. coli* DH5α by chemical transformation. The cloned gene sequence was confirmed and then transferred to the expression vector pASG IBA 33 and finally transferred to *E. coli* BL21-DE3. The colonies harboring the plasmid were used for overproduction of the protein.

Purification of Flavodoxin—*E. coli* cells overproducing the recombinant flavodoxin (10 g of wet mass) were suspended in 50 mM potassium phosphate/150 mM NaCl, pH 7.0 (buffer A) and disrupted by three passages through a French press at 140 MPa. Cell debris and membranes were separated by centrifugation at 150,000 × *g* for 45 min at 4 °C to obtain a membrane-free extract. The extract was passed through a 45-μm filter and loaded on a 5-ml Ni-Sepharose column (HiTrap, GE Healthcare, München, Germany), which was pre-equilibrated with buffer A. All purification steps were performed at 4 °C, unless otherwise mentioned. After loading the membrane-free extract, the column was washed with 10 column volumes of buffer A to remove contaminating proteins. The protein was eluted with 250 mM imidazole in buffer A. The purified protein was desalted and concentrated; FMN in molar excess was added and incubated overnight in the dark at 4 °C. Chromatography on a Superdex 75 pg (GE Healthcare) yielded homogenous protein and removed excess FMN. The protein was stored at −80 °C until use.

Purification of Ferredoxin—The purification was performed under strict anoxic conditions under an atmosphere of 95% N_2 and 5% H_2 (Coy Anaerobic Chamber) (14). Frozen *C. tetanomorphum* cells (10 g) were suspended in 50 mM potassium phosphate, pH 6.8 (buffer B), and passed three times through a French press at 140 MPa. The supernatant obtained by centrifugation at 150,000 × *g* for 1 h at 4 °C was loaded on a DEAE column, which was pre-equilibrated by buffer B. The column was washed with 2 column volumes of buffer B, and the protein

was eluted with a gradient of 0–100% 1 M NaCl achieved over 10 column volumes (600 ml). Active fractions of ferredoxin, identified by the bifurcation assay (see below), were pooled and concentrated by ultrafiltration with a 3-kDa membrane (Centricon, Merck Millipore, Darmstadt, Germany). The concentrated protein sample was chromatographed on a Superdex 75 column pre-equilibrated with 150 mM NaCl in buffer B. The fractions containing ferredoxin were identified by their dark brown color, concentrated, and stored at −80 °C under anaerobic conditions. The ferredoxin concentration was measured by its iron content (14), and a molecular mass of 6 kDa was used. The concentrations of flavodoxin and ferredoxin in *A. fermentans* cells listed as μmol/g of protein (14) were converted to mM by assuming a cell volume of 2.5 ml/g of protein (20).

Preparation of Hydrogenase—Frozen *C. pasteurianum* cells (5 g) were suspended in 10 ml of buffer B and broken by three passages through a French press at 140 MPa (20,000 p.s.i.) under strict anoxic conditions. The broken cells were centrifuged at 7,000 × *g* for 20 min. The supernatant was heated to 55–60 °C for 10–15 min under a hydrogen atmosphere. Afterward the extract was cooled in ice for 30 min. The precipitated proteins were removed by centrifugation at 20,000 × *g* for 30 min. The supernatant containing hydrogenase was stored at −80 °C until use (21).

Electron-transferring Flavoprotein and Butyryl-CoA Dehydrogenase—Recombinant Etf from *A. fermentans* with a C-terminal His tag at the α-subunit produced in *E. coli* and native Bcd from *A. fermentans* were prepared as reported earlier (10). Both proteins were incubated with excess FAD overnight in dark at 4 °C. Excess FAD was removed by using a desalting PD 10 column (GE Healthcare). The FAD content of the proteins was calculated using $\epsilon_{450} = 11.3\ mM^{-1}\ cm^{-1}$.

Preparation of Membrane Extracts—Wet-packed cells of *A. fermentans* (20 g) were suspended in buffer B and broken by four passages through a French press at 140 MPa under strict anoxic conditions. Cell debris was removed by centrifugation 20,000 × *g* for 20 min at 4 °C. The crude extract was centrifuged at 150,000 × *g* for 60 min. The supernatant was stored for further purification of soluble proteins, and the membrane pellet was homogenized and washed twice with buffer B by centrifuging at 150,000 × *g* for 30 min. The obtained inverted vesicles were used for Na^+/Li^+ dependence assays. For other kinetic measurements, the vesicles were solubilized with 2% *n*-dodecyl-β-D-maltoside in buffer B supplemented with 0.5 M NaCl and then well homogenized. The homogenate was kept on ice for 30 min and centrifuged at 150,000 × *g* for 30 min. The supernatant was used for the experiments (16).

Analytical Methods—Protein concentrations were estimated with the Bradford assay (22) (Bio-Rad-Microassay reagent, Bio-Rad Laboratories, Munich, Germany). Bovine serum albumin (Sigma, Darmstadt, Germany) was used as standard. SDS-PAGE was performed as described (23). All enzyme assays were performed under an atmosphere of 95% N_2 and 5% H_2. The bifurcation assay, *i.e.* the measurement of the reduction of crotonyl-CoA to butyryl-CoA, was done in a quartz cuvette (total volume 500 μl, $d = 1$ cm) using, unless otherwise indicated, 0.5 μM Etf_{Af}, 1 μM Bcd_{Af}, 1 μM ferredoxin, 30 μg of crude hydrogenase, and 250 μM NADH in buffer B. The reaction was started with 100 μM crotonyl-CoA. The decrease in NADH concentration was monitored at 340 nm, $\epsilon = 6.3\ mM^{-1}\ cm^{-1}$ (24). Stoichiometric amounts of flavodoxin (50 μM) were used in place of ferredoxin/hydrogenase and monitored at 340 nm and also at 450 nm (oxidized flavin) and 578 (blue flavin semiquinone). Usually all measurements were repeated three times and the error bars (average with S.D.) were inserted into the figures when appropriate.

Determination of Na and Other Elements—After running the bifurcation/Rnf reaction, the whole assay was analyzed by inductively coupled plasma mass spectrometry (ICP-MS). The protein samples and buffer blanks were diluted 100-fold with ultrapure water and spiked with 10 μg yttrium (^{89}Y)/kg as internal standard. The calibration of the ICP-MS was performed in the concentration range 0.1–100 μg/kg using dilutions of a Merck ICP multi-element standard solution IV (Merck product number 111355). The elemental contents of Li, Na, Mg, K, Mn, Fe, Co, Ni, Cu, and Zn in the protein sample were determined by ICP-MS using an Agilent 7900 ICP-MS with HEN nebulizer and cooled Scott spray chamber under standard operating conditions. The instrument was auto-tuned to robust plasma conditions to avoid matrix effects. The isotopes ^7Li, ^{23}Na, ^{24}Mg, ^{26}Mg, ^{39}K, ^{55}Mn, ^{56}Fe, ^{57}Fe, ^{59}Co, ^{60}Ni, ^{62}Ni, ^{63}Cu, ^{65}Cu, ^{64}Zn, ^{66}Zn and ^{67}Zn were measured under NoGas, He collision, and H_2 reaction mode conditions. Some isotopes were strongly interfered from the K-containing matrix (mainly ^{55}Mn) in the NoGas mode and therefore rejected. The assay used to determine the dependence of Na contained 43 ± 1 μM Na, which was mainly introduced by the 50 mM potassium phosphate buffer, pH 6.8. In addition, about 8 μM Mg, 2.5 μM Fe, 0.8 μM Ni, and 2 μM Zn were detected.

Results

Characterization of Recombinant Flavodoxin from A. fermentans—The flavodoxin with a C-terminal His tag was affinity-purified from a cell lysate of *E. coli* BL21 (DE3) harboring the pASG IBA33 vector with the flavodoxin gene as described under "Materials and Methods." To assess its homogeneity, the protein was subjected to gel filtration at pH 7.0 whereby several peaks were observed. Each of the two most prominent peaks, when analyzed by SDS-PAGE, revealed a single band around the 15-kDa protein marker. Both proteins were identified to be flavodoxin by peptide mapping with MALDI-TOF mass spectrometry, showing that the flavodoxin tends to make a mixture of oligomeric and monomeric forms. The molecular mass of the monomeric form (15.37 kDa) fits to the calculated value based on the amino acid sequence from the protein (14.54 kDa) and the His tag (0.84 kDa). The UV-visible spectrum of the purified flavodoxin (Fig. 1) exhibited the two characteristic peaks at 375 and 448 nm with a shoulder at 464 nm. The flavodoxin was heated at 80 °C for 5 min, and the yellow compound in the supernatant of the precipitated protein was identified as FMN by TLC and reverse phase HPLC. The FMN content of the protein was quantified by using the known absorbance coefficients at $\lambda = 450$ nm ($\epsilon = 11.3\ mM^{-1}\ cm^{-1}$) and $\lambda = 375$ nm ($\epsilon = 10.7\ mM^{-1}\ cm^{-1}$) (25). Flavodoxin as isolated contained only 0.2 mol of FMN per monomer, which was raised to 0.5–0.6 upon overnight incubation with a molar

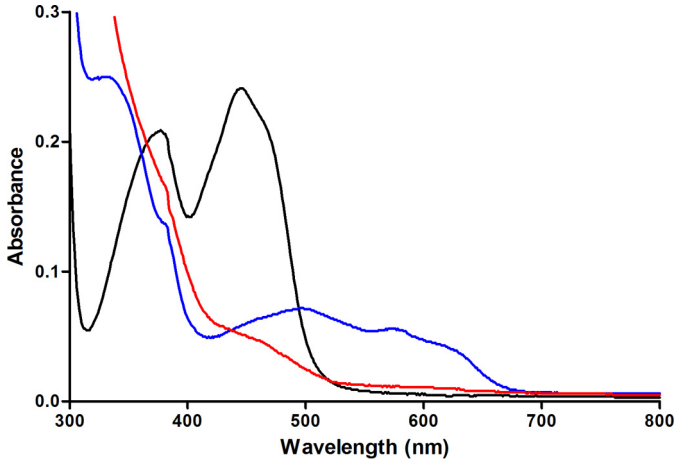

FIGURE 1. **Reduction of flavodoxin by Ti(III) citrate.** *Black trace*, oxidized Fld; *blue trace*, semiquinone FldH$^{\bullet}$ reduced by 0.1 mM Ti(III)citrate; *red trace*, completely reduced FldH^{-} by 5 mM Ti(III)citrate.

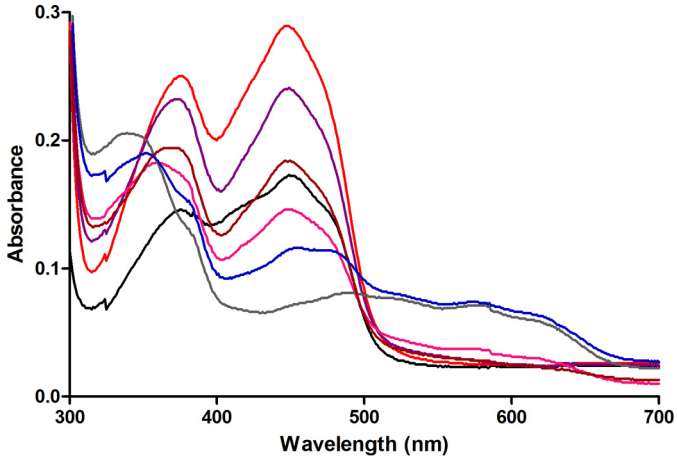

FIGURE 2. **Titration of Etf and flavodoxin with NADH.** *Black spectrum* (A_{450} = 0.17), 10 μM Etf containing 13 μM FAD. *Red spectrum* (A_{450} = 0.30), after the addition of 20 μM flavodoxin containing 10 μM FMN. This mixture was reduced stepwise with NADH: *purple trace* (A_{450} = 0.24), 5 μM NADH; *brown trace* (A_{450} = 0.18), 10 μM; *pink trace* (A_{450} = 0.14), 12.5 μM; *blue trace* (A_{450} = 0.12), 15 μM; *gray trace* (A_{450} = 0.08), 20 μM.

excess of FMN in the dark at 4 °C followed by gel filtration to remove the unbound FMN. In contrast, the FMN content of the flavodoxin purified from *A. fermentans* was reported to be 1.0 mol/mol of protein (15), which suggests that upon overproduction in *E. coli*, about half of the recombinant flavodoxin folded into a structure unable to bind FMN, which could be due to the presence of the His tag. The production of flavodoxin from *Anabaena* without a tag in *E. coli* yielded pure holo-flavodoxin with a ratio of A_{465}/A_{274} = 0.17 (26), whereas the ratio of A_{465}/A_{274} obtained with the recombinant protein in this study was 0.146. The addition of 0.1 mM Ti(III)citrate to 35 μM flavodoxin (22 μM FMN) at pH 6.8 reduced the absorbance at 375 and 446 nm, and two new stable peaks at 500 and 578 nm appeared (Fig. 1), which are characteristic for the blue neutral semiquinone (FldH$^{\bullet}$) (27). Upon increasing the concentration of Ti(III)citrate to 5 mM, both peaks disappeared and the spectrum changed to that of completely reduced flavodoxin (FldH^{-}).

Etf Exhibits Low Diaphorase Activity—Upon incubation of flavodoxin with NADH, the absorbance at 450 nm remained unchanged. In the presence of Etf, however, flavodoxin was slowly reduced by NADH to the blue semiquinone. As shown in Fig. 2, stepwise addition of 2.5 μM NADH to a mixture of 10 μM Etf (13 μM FAD) and 20 μM flavodoxin (10 μM FMN) reduced the 450 nm peak. The lower peak at 375 nm shifted to 370 nm and decreased more slowly until the height of both peaks became equal (about 7.5–10 μM NADH), indicating the known formation of the red anionic semiquinone of the α-FAD of Etf (28, 29). At 12.5 μM NADH, the blue neutral semiquinone of flavodoxin began to appear and was fully present at 15 μM NADH: theoretical at 13 + 0.5 × 10 = 18 μM NADH. At ≥17.5 μM NADH, a peak at 340 nm became visible due to excess of NADH. Hence Etf catalyzes the slow reduction of flavodoxin to the semiquinone by NADH, which is called diaphorase activity: specific activity 0.04 units (mg of Etf)$^{-1}$.

Electron Bifurcation Reduces Flavodoxin to the Hydroquinone—Due to the low redox potential of the semiquinone/hydroquinone couple ($E^{\circ\prime}$ = −430 mV), NADH can reduce flavodoxin only to the semiquinone ($E^{\circ\prime}$ = −60 mV). With electron bifurcation, however, the low potential can easily be achieved. To study the reduction of flavodoxin during the electron bifurcation process, catalytic amounts of electron-bifurcating flavoprotein from *A. fermentans* (Etf_{Af}; 0.5 μM) and butyryl-CoA dehydrogenase (Bcd_{Af}; 1.0 μM subunit), 125 μM NADH, and 75 μM flavodoxin (43 μM FMN) were mixed under strict anaerobic conditions, and the UV-visible spectrum of the oxidized Fld was obtained. Upon the addition of 30 μM crotonyl-CoA, the peak at 450 nm decreased and that of the blue semiquinone (FldH$^{\bullet}$) at 578 nm, which remained stable for more than 3 min, became visible. Upon further addition of 50 μM crotonyl-CoA, the semiquinone was reduced to the hydroquinone (FldH^{-}). The complete reduction of flavodoxin indicated that an effective redox potential of $E_2' \leq -500$ mV was reached. The same behavior was observed in the bifurcation process with ferredoxin (6, 29). To get more insight into the kinetics of this reduction, we simultaneously measured the absorbance changes with time at three different wavelengths, NADH at 340 nm, quinone at 450 nm, and semiquinone at 578 nm (Fig. 3). After starting the incubation of Etf, Bcd, flavodoxin, and NADH with crotonyl-CoA, we observed NADH oxidation, quinone reduction, and semiquinone formation. Only after the quinone was quantitatively reduced to the semiquinone did an ~1.4 times faster reduction to the hydroquinone take place. At this point, the apparent rate of NADH consumption increased accordingly. This result showed that the thermodynamically more facile reduction of the quinone to the semiquinone ($E_1^{\circ\prime}$ = −60 mV) occurred first and was followed by the more difficult reduction to the hydroquinone ($E_2^{\circ\prime}$ = −430 mV) (15). In contrast, the rates of the two reductions did not follow the thermodynamics, indicating that at the Etf, the semiquinone is a better electron acceptor than the quinone.

Hydrogenase Catalyzes the Reoxidation of Flavodoxin Hydroquinone—In our previous bifurcation assays, the hydrogenase from *C. pasteurianum* recycled oxidized ferredoxin concomitant with hydrogen formation (6, 29). With 100 μM NADH, 50 μM crotonyl-CoA, 0.5 μM Etf, and 1.0 μM Bcd (optimal Etf/Bcd ratio) from *A. fermentans*, specific activities up to V_{max} = 3.2 units (mg of Etf)$^{-1}$ were achieved. The apparent K_m

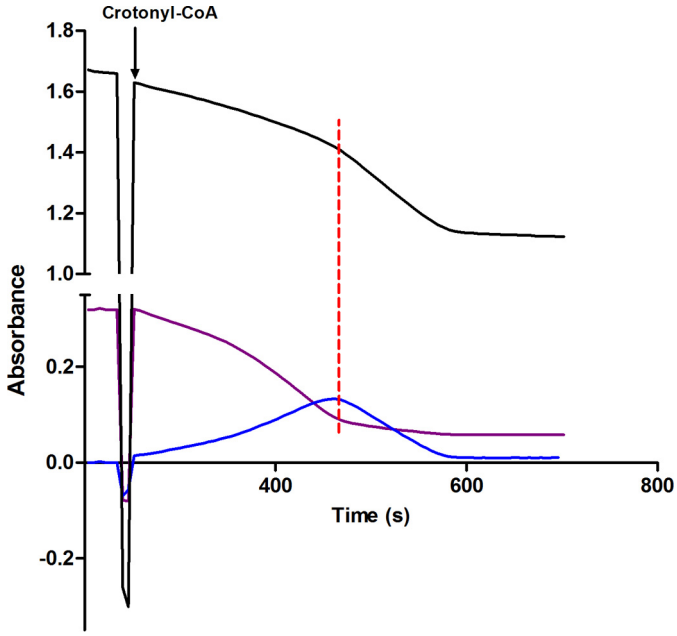

FIGURE 3. **Kinetics of the reduction of flavodoxin.** To an incubation with 0.5 μM Etf and 1 μM Bcd was added 250 μM NADH at $t = 50$ s and 50 μM Fld (29 μM FMN) at $t = 150$ s. The reaction was started with 75 μM crotonyl-CoA at $t = 250$ s and measured simultaneously at three wavelengths: 340 nm, *black trace*; 450 nm, *purple trace*; 578 nm, *blue trace*.

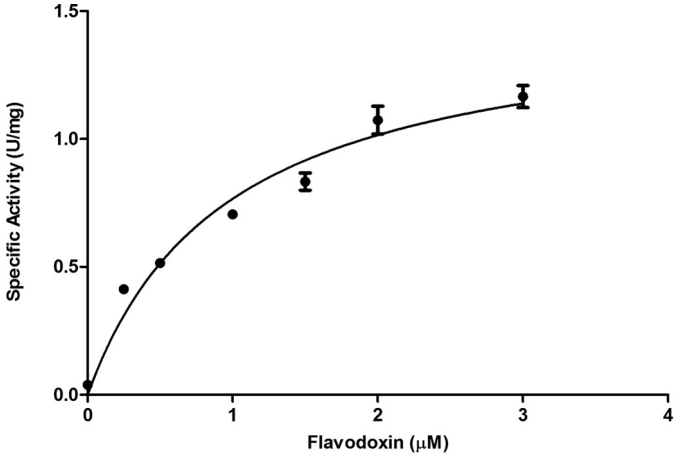

FIGURE 4. **Rate of NADH oxidation (units (mg of Etf)$^{-1}$) as a function of Fld concentration.** The cuvette contained 0.5 μM Etf, 1.0 μM Bcd, 100 μM NADH, and hydrogenase. *Error bars* indicate ± S.D.

for ferredoxin was determined as 0.26 ± 0.03 μM (10). This system worked equally well with Fld, exhibiting a similar V_{max} = 1.2 units (mg of Etf)$^{-1}$ and an apparent K_m = 0.42 ± 0.05 μM, based on a content of 0.5 FMN/Fld (Fig. 4). Initially, Fld is reduced to the hydroquinone ($FldH^-$, Reaction 1). In the next step, the hydrogenase catalyzes the oxidation of $FldH^-$ to the semiquinone ($FldH^{\cdot}$, Reaction 2), because further oxidation to the quinone (Fld) is not possible due to the much more positive redox potential of $E^{\circ\prime} = -60$ mV than that of hydrogen, $E^{\circ\prime} = -414$ mV. $FldH^{\cdot}$ is reduced again to $FldH^-$ by electron bifurcation (Reaction 3). In summary, crotonyl-CoA and 2 protons are reduced with 2 NADH to butyryl-CoA and hydrogen (Reaction 4), whereby flavodoxin cycles between the semiquinone and hydroquinone states. The same stoichiometry (2 NADH/

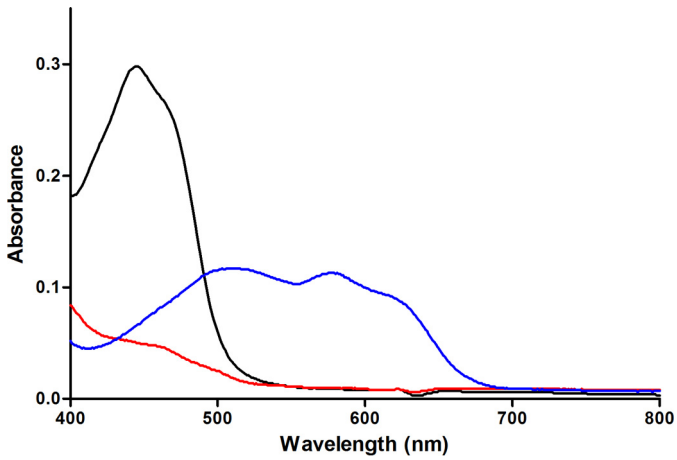

FIGURE 5. **Reduction of flavodoxin by electron bifurcation and reoxidation by NAD$^+$ mediated by Rnf.** *Black trace*, spectrum of 50 μM flavodoxin. The addition of 0.5 μM Etf, 1.0 μM Bcd, 250 μM NADH, and 100 μM crotonyl-CoA reduced Fld to $FldH^-$ (Reaction 1) (*red trace*). Subsequent addition of Rnf caused the oxidation $FldH^-$ to $FldH^{\cdot}$ by the formed NAD^+ (Reaction 5). The reaction cycled until the excess NADH had consumed all crotonyl-CoA, yielding the spectrum of the pure $FldH^{\cdot}$ (*blue trace*).

crotonyl-CoA) was observed earlier with ferredoxin (29). At the end of the reaction when crotonyl-CoA and/or NADH are consumed, the semiquinone cannot be reduced anymore (Reaction 3).

$$\text{Etf} + \text{Bcd: Crotonyl-CoA} + 2\ \text{NADH} + \text{Fld} + 2\ \text{H}^+ \rightarrow \text{Butyryl-CoA} + 2\ \text{NAD}^+ + \text{FldH}^-$$

Reaction 1

$$\text{Hydrogenase: } 2\ \text{FldH}^- + 2\ \text{H}^+ = 2\ \text{FldH}^{\cdot} + \text{H}_2$$

Reaction 2

$$\text{Etf} + \text{Bcd: Crotonyl-CoA} + 2\ \text{NADH} + 2\ \text{FldH}^{\cdot} \rightarrow \text{Butyryl-CoA} + 2\ \text{NAD}^+ + 2\ \text{FldH}^-$$

Reaction 3

$$\text{Sum (2 + 3): Crotonyl-CoA} + 2\ \text{NADH} + 2\ \text{H}^+ \rightarrow \text{Butyryl-CoA} + 2\ \text{NAD}^+ + \text{H}_2$$

Reaction 4

Rnf Mediates the Reoxidation of Either Flavodoxin Hydroquinone or Reduced Ferredoxin—Membranes of *A. fermentans* solubilized with dodecylmaltoside contain a very active Rnf that catalyzes the exergonic oxidation of NADH with ferricyanide, specific activity = 20 units (mg of protein)$^{-1}$ (8, 30, 31). Now electron bifurcation allowed the complete reduction of ferredoxin or flavodoxin, with which the reaction could be measured in the physiologic direction with the natural electron donor (Reaction 5 with flavodoxin) (Fig. 5). Together with Reaction 3, the simple Reaction 6 for the reduction of crotonyl-CoA to butyryl-CoA by NADH was obtained. This stoichiometry could be verified experimentally (1.09 NADH/crotonyl-CoA, Fig. 6).

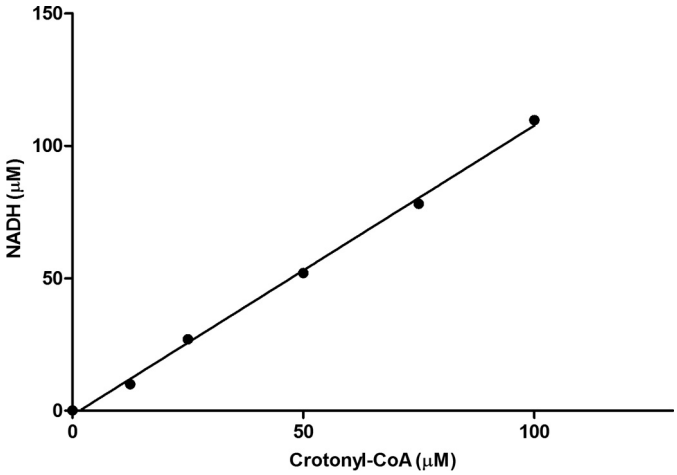

FIGURE 6. **Stoichiometry of consumed NADH as a function of the added crotonyl-CoA according to Reaction 6.** The assays contained 250 μM NADH, 0.5 μM Etf, 1.0 μM Bcd, 5 μM Fld, and 35 μg of solubilized membrane protein from *A. fermentans* as source of Rnf; S.D. was ±2%.

$$\text{Rnf: } 2\ \text{FldH}^- + \text{NAD}^+ + \text{H}^+ \rightarrow 2\ \text{FldH}^{\cdot} + \text{NADH}$$

Reaction 5

$$\text{Sum (3 + 5): Crotonyl-CoA} + \text{NADH} + \text{H}^+ \rightarrow \text{butyryl-CoA} + \text{NAD}^+$$

Reaction 6

In this system, the apparent $K_m = 2.0 \pm 0.4$ μM flavodoxin and $V_{max} = 1.1$ units (mg of Etf)$^{-1}$ as well as $K_m = 1.4 \pm 0.1$ μM ferredoxin and $V_{max} = 1.3$ units (mg of Etf)$^{-1}$ were measured. At the end of the reaction, when either NADH or crotonyl-CoA was consumed, flavodoxin was quantitatively converted to the semiquinone as shown in Fig. 5, *blue trace*. This figure exhibits the UV-visible spectrum of the blue semiquinone of flavodoxin between 400 and 700 nm with two peaks around 510 and 580 nm.

Sodium Dependence of Rnf—It was postulated that Rnfs from *A. fermentans* and many clostridia use the energy difference of about 200 mV between reduced ferredoxin or flavodoxin and NADH to generate an electrochemical Na^+ gradient for ATP synthesis (7, 8) as shown recently for Rnf from *Acetobacterium woodii* (9, 32). Using inverted membrane vesicles from *C. tetanomorphum* and *A. fermentans* in two assays, with either NADH or Ti(III) citrate + ferredoxin as donor and ferricyanide or NAD^+ as acceptor, respectively, a scalar Na^+ dependence could be not be detected. Furthermore, when the pH was raised above 7.0, Ti(III) citrate reduced NAD^+ directly in the absence of ferredoxin and Rnf (30). In the reaction with inverted membrane vesicles from *A. fermentans*, Etf, Bcd, flavodoxin, NADH, and crotonyl-CoA (Reaction 6), a sodium or lithium ion dependence could indeed be observed (Fig. 7). For the determination of the apparent $K_m = 120 \pm 20$ μM Na^+ or 275 ± 50 μM Li^+, the Na^+ concentrations of the assays before the addition of defined amounts of NaCl or LiCl were measured with ICP-MS. The lowest Na^+ concentration in the assay mixture was 43 μM, whereas that of Li^+ was close to zero.

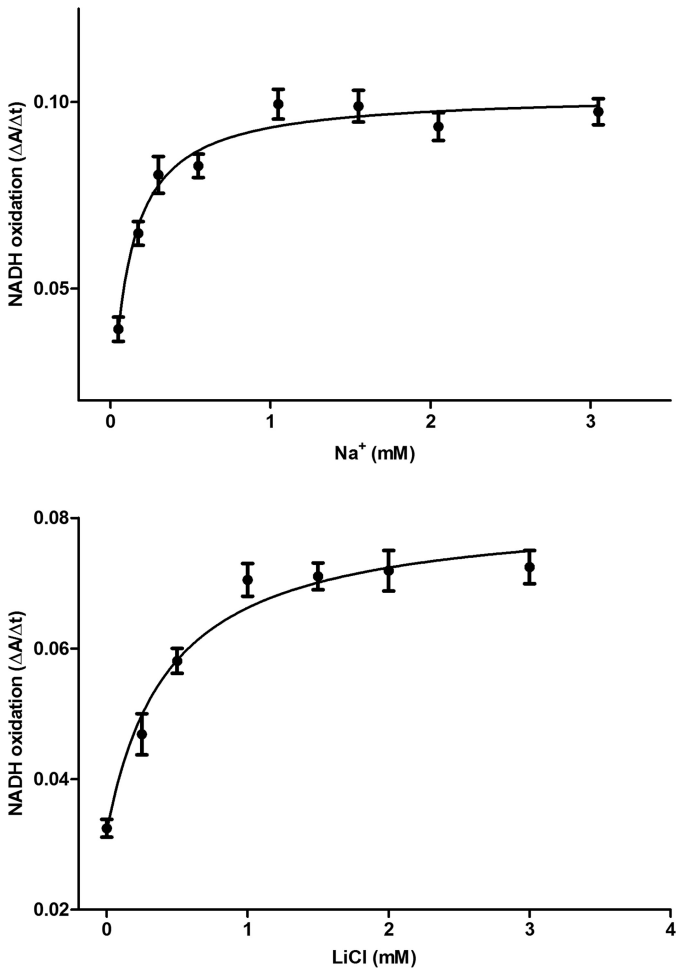

FIGURE 7. **Requirement of Na^+ or Li^+ for Rnf activity.** Shown are the rates of NADH oxidation ($\Delta A_{340}/\Delta t$) according to Reaction 6 in the presence of 250 μM NADH, 100 μM crotonyl-CoA, 0.5 μM Etf, 1.0 μM Bcd, 5 μM Fld, and 50 μg of membrane vesicles from *A. fermentans* as the source of Rnf. The data were fitted by the modified Michaelis-Menten equation: $v = V_{max} \times (X + X_0) \times (K_m + X + X_0)^{-1}$, where X signifies the concentrations of Na^+ or Li^+ added and X_0 signifies the concentration of Na^+ = 0.043 mM already present in the assay mixes. *Error bars* indicate ± S.D.

Discussion

Our results clearly demonstrate that flavodoxin can replace ferredoxin as acceptor in the Etf + Bcd bifurcating system of *A. fermentans*, as donor of the [FeFe]hydrogenase of *C. pasteurianum*, and as donor/acceptor of the Rnf of *A. fermentans*. Thus flavodoxin or its semiquinone is reduced by NADH to the hydroquinone via electron bifurcation and reoxidized back to the semiquinone catalyzed either by the hydrogenase or by RnfABCDGE (*Acfer_0108-0113*) (19). The advantage of studying these reactions with flavodoxin is the facile identification of the blue neutral semiquinone, whereas with ferredoxin, the Fd, Fd^-, and Fd^{2-} states are not easily differentiated. Thus it could be shown that the quinone was almost quantitatively reduced to the semiquinone before it was further reduced to the hydroquinone as expected from thermodynamics (Fig. 3). In contrast, the reduction of the flavodoxin semiquinone to the hydroquinone proceeded ~1.4 times faster than the reduction of the quinone to the semiquinone. Hence a one-electron transfer to a compound with an unpaired electron most likely proceeds over

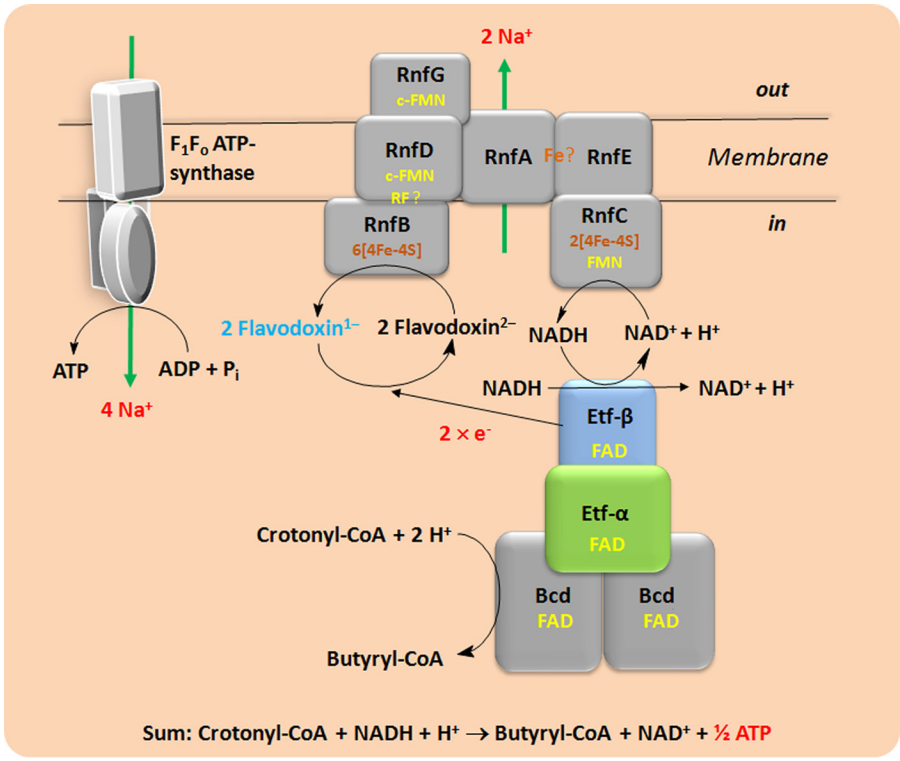

FIGURE 8. **Proposed sodium ion gradient phosphorylation driven by the reduction of crotonyl-CoA in *A. fermentans*.** The whole picture is a modification of that taken from Ref. 9. The presence of an F_1F_o ATP synthase was deduced from the genome of *A. fermentans*. The model of Rnf was constructed from data obtained from Rnf of *C. tetanomorphum* (30) and NADH-quinone oxidoreductase (Nqr) of *V. cholerae* (33). For the structure of the Etf-Bcd complex see Ref. 10.

a lower barrier than the addition of one electron to a closed shell. Alternatively, the easier one-electron reduction of the semiquinone could be an adaption to the physiologic conditions under which flavodoxin cycles between semiquinone and hydroquinone, whereas the quinone hardly exists.

In this work, we showed for the first time that Rnf from *A. fermentans* indeed required Na^+ for activity. The failure of earlier attempts to verify this effect was certainly due to the application of artificial electron acceptors and donors. The heterohexameric Rnf from *C. tetanomorphum* contains riboflavin, non-covalently bound riboflavin-5′-phosphate, two riboflavin-5′-phosphates covalently bound to RnfG and RnfD, about five iron-sulfur clusters (30), and probably one iron atom coordinated by RnfA and RnfE as in the homologous NADH-quinone oxidoreductase (Nqr) of *Vibrio cholerae* (33) (Fig. 8). Thus one of this plethora of cofactors could transfer an electron directly to ferricyanide or accept one electron from Ti(III)citrate without passing the Na^+-translocating site. Here we used electron bifurcation for the generation of flavodoxin hydroquinone (Fld^{2-}) in the absence of Ti(III)citrate and were able to demonstrate the Na^+ and the Li^+ dependences of Rnf from *A. fermentans*. The apparent K_m value of 120 ± 20 μM Na^+ at pH 6.8 is similar to those of Rnf from *A. woodii* with K_m values of 201 ± 30 μM Na^+ at pH 6 and 155 ± 39 μM at pH 7.7 (34). The K_m values for Li^+ also lie in the same range for both Rnfs. Surprisingly, these values are much lower than those of the biotin-containing Na^+ pumps glutaconyl-CoA decarboxylase from *A. fermentans* (35) or oxaloacetate decarboxylase from *Klebsiella pneumoniae* (36), which exhibit apparent K_m values of 1.0–1.5 mM Na^+ and 25–100 mM Li^+.

The now confirmed Na^+ dependence of Rnf fits well to the Na^+ bioenergetics of *A. fermentans* (Fig. 8). This organism ferments glutamate via the radical dehydration of (*R*)-2-hydroxyglutaryl-CoA (37) followed by the Na^+-dependent decarboxylation of the product glutaconyl-CoA to crotonyl-CoA (35, 38). Disproportionation of crotonyl-CoA yields acetate, butyrate, and hydrogen; the latter stems from reduced flavodoxin or ferredoxin generated by electron bifurcation with crotonyl-CoA and NADH. The Na^+-pumping enzymes of this organism are glutaconyl-CoA decarboxylase and Rnf, both of which most likely translocate two Na^+ per turnover. According to the proposed pathway of glutamate fermentation, the decarboxylase contributes 2 Na^+/glutamate and Rnf adds 2 Na^+/5 glutamate (7). Because 1 Na^+/glutamate is most likely required for the import, from 2 + 0.4 − 1 = 1.4 Na^+/glutamate are left for the Na^+-dependent ATP synthase, leading to 1.4/4 = 0.35 ATP/glutamate via ion gradient phosphorylation. The contribution of substrate level phosphorylation amounts to 3 ATP/5 glutamate, which sums up to 0.95 ATP/glutamate, the maximum theoretical yield (7).

The electron-bifurcating Etf + Bcd system has been shown to provide a stable steady state concentration of almost completely reduced ferredoxin or flavodoxin ($E' \leq -500$ mV). Thus in addition to hydrogenase and Rnf, this system also allows us to study other enzymatic reactions in which these reduced electron carriers are substrates. The reaction rates are easily followed via the oxidation of NADH. Examples are the synthases that form 2-oxo acids from acyl-CoA and CO_2, such as pyruvate synthase, or the tungsten-containing aldehyde dehydrogenases, which are also proposed to catalyze the reverse reactions, the reduction of free carboxylic acids to aldehydes. Further-

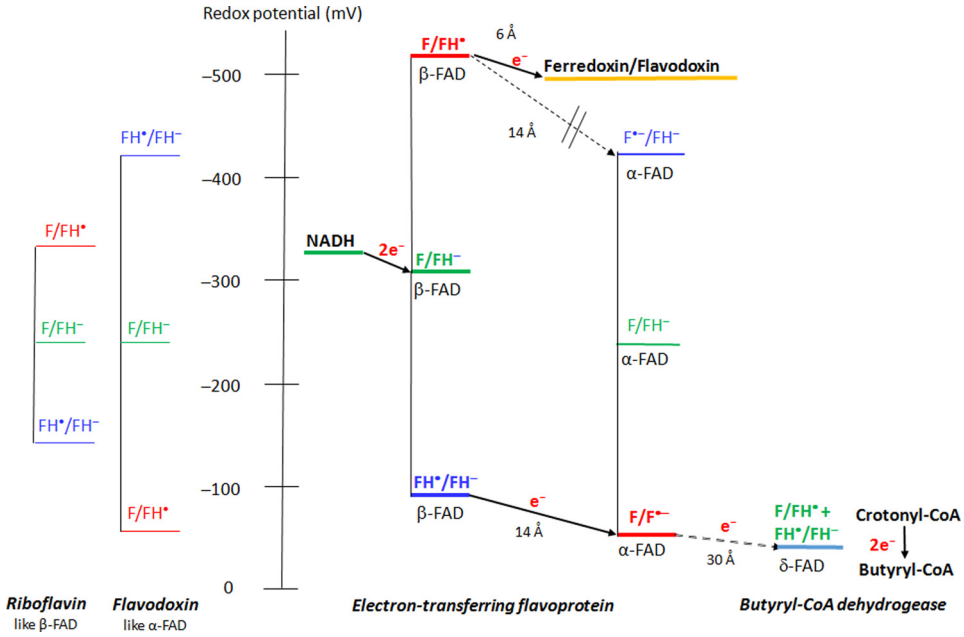

FIGURE 9. **Proposed mechanism of electron bifurcation as deduced from the redox potentials of riboflavin and flavodoxin.** The *bold lines and letters* indicate the postulated one-electron flows, endergonic from NADH to ferredoxin or flavodoxin and exergonic to crotonyl-CoA. See "Discussion" for further details.

more, the Etf + Bcd system enables us to monitor even very difficult conversions such as nitrogen fixation or benzoyl-CoA reduction just by NADH oxidation at 340 nm.

Stimulated by the inverted redox potentials of flavodoxin as compared with those of free FAD or riboflavin (39), we propose a mechanism of electron bifurcation with Etf + Bcd (Fig. 9). Crystallographic studies showed that α-FAD of Etf from *A. fermentans* is bound to domain II of the α-subunit with a flavodoxin-like fold (10). The similarity α-FAD with flavodoxin is manifested by the ability of both proteins to stabilize a semiquinone, a red anionic semiquinone in the case of α-FAD and the protonated blue form in the case of flavodoxin. The formation of stable semiquinones is due to the inverse redox potentials of flavodoxin (see above) and α-FAD. The redox potentials of α-FAD in the Etf from *M. elsdenii* (Etf_{Me}), a bacterium closely related to *A. fermentans*, have been reported as $E^{\circ\prime}{}_1 = +81$ mV for α-FAD/FAD$^{\bullet-}$ and $E^{\circ\prime}{}_2 = -136$ mV for α-FAD$^{\bullet-}$/FADH (28). Although both potentials are much higher than the corresponding potentials of flavodoxin (−60 and −430 mV, respectively), there are indications that they decrease considerably when Etf forms a complex with Bcd as assumed in Fig. 9 (10, 40). Otherwise the reduction of crotonyl-CoA to butyryl-CoA ($E^{\circ\prime} = -10$ mV) by α-FAD$^{\bullet-}$ would be difficult. Upon titration of Etf with ½ NADH (¼ NADH/FAD), the stable red semiquinone anion ($\lambda_{max} = 370$ nm), whose concentration is significantly increased in the presence of Bcd (10), is observed (see Fig. 2 and Ref. 28). A special feature of α-FAD is an internal hydrogen bond between the 4′-OH of its ribityl side chain to either N1 or to the C2=O group of the isoalloxazine ring. This bond, as well as several other interactions with the surrounding amino acid residues, perturbs the UV-visible spectrum of α-FAD in such a way that an extra absorption band around 400 nm between the two prominent peaks of the FAD quinone at 375 and 446 nm is observed. This band at 400 nm is quenched by reduction of Etf with NADH in a 1:1 ratio, whereby the remaining still oxidized β-FAD exhibits a normal flavin spectrum. This spectrum is also obtained when the α-FAD is removed by treatment of the Etf with KBr (28, 29).

β-FAD is tightly bound to Etf between domain III, the β-subunit, and domain I of the α-subunit. It exhibits a more closed conformation, different from that of α-FAD and without the internal hydrogen bond. Therefore we conclude that the redox potentials of β-FAD are not reversed and similar to those of free riboflavin. Unfortunately, only the two-electron redox potential of the related Etf from *M. elsdenii* could be measured as $E^{\circ\prime} = -279$ mV for β-FAD/FADH$^-$ (28). Together with the one-electron redox potentials of riboflavin (Rf), $E^{\circ\prime}{}_{Rf1} = -314$ mV for Rf/RfH$^\bullet$ and $E^{\circ\prime}{}_{Rf2} = -124$ mV for RfH$^\bullet$/RfH$^-$ (39), the real redox potentials of β-FAD could be $E^{\circ\prime}{}_\beta = -279 \pm ½(E^{\circ\prime}{}_{Rf1} - E^{\circ\prime}{}_{Rf2}) = -374$ mV and −184 mV. Due to interaction with the protein, the separation between $E^{\circ\prime}{}_{\beta1}$ and $E^{\circ\prime}{}_{\beta2}$ could be even larger, which is assumed in Fig. 9.

Using these estimated redox potentials for α- and β-FAD, one can construct a possible mechanism for electron bifurcation. As shown by crystallographic studies, NADH binds close to β-FAD and reduces it to β-FADH$^-$ (29). Due to the ability of α-FAD to stabilize a semiquinone, only one electron is shifted from the low β-FADH$^\bullet$/FADH$^-$ level (about −90 mV, Fig. 9) to α-FAD/FAD$^{\bullet-}$ (about −60 mV), which is 14 Å apart. According to the law of energy conservation, the other electron at the β-FAD/FADH$^\bullet$ level becomes "red hot" (about −520 mV) (41) and reduces the much more closely located ferredoxin that is only 6 Å apart (29). Because the isoalloxazine ring of FMN sits on the surface of flavodoxin, an electron from β-FADH$^\bullet$ to this acceptor probably has to pass the same distance. Now the flexible domain II carrying α-FAD$^{\bullet-}$ must undergo a large conformational change to interact with δ-FAD of Bcd, which, in the complex of human Etf and medium chain acyl-CoA dehydrogenase, has been shown to be 30 Å apart (42). After reduction of δ-FAD to the semiquinone (δ-FADH$^\bullet$), a second round of bifurcation generates δ-FADH$^-$ that transfers a hydride to crotonyl-

CoA, yielding butyryl-CoA. Alternatively, δ-FADH$^{\bullet}$ reduces crotonyl-CoA to an allylic ketyl radical (43, 44), and the second δ-FADH$^{\bullet}$ completes the reduction to butyryl-CoA.

This mechanism is actually similar to that of the "redox seesaw" originally proposed by Peter Mitchell (41, 55), although the redox potentials of the bifurcating β-FAD are normal and not inverted. The inverted redox potentials of α-FAD are necessary to generate the high potential one-electron acceptor able to form a stable semiquinone, which has to be transported over 30 Å to δ-FAD of Bcd. Other bifurcating systems use iron sulfur clusters as high potential electron acceptors; established cases are the Rieske [2Fe-2S] cluster in the Q-cycle of complex III of the respiratory chain (45) and the [4Fe-4S] cluster N3 close to FMN of NADH-quinone oxidoreductase (Nuo, complex I) (46). The Rieske [2Fe-2S] cluster has a function very similar to that of α-FAD. It accepts the high potential electron from ubihydroquinone (UQH_2) and swings over to cytochrome c_1, which becomes reduced. It has been proposed that in complex I, the two electrons of $FMNH^-$ bifurcate; one goes to the high potential [4Fe-4S] cluster N3, and the other goes to the lower potential [2Fe-2S] cluster N1a. Although the electron on N3 moves forward via six additional clusters to the ubiquinone, the other electron is stored on N1a until the way is free to follow the first electron. Thus the formation of a reactive oxygen species-forming FMNH$^{\bullet}$ is avoided (46). With the exception of Etf + Bcd, all other bifurcating systems also contain iron-sulfur clusters, which possibly serve as high potential electron acceptors (47–54). Probably these clusters can be more easily tuned to the required redox potentials than flavins. Hence the Etf + Bcd system appears to be a special case among the bifurcating flavoprotein complexes, in which the flavodoxin-like α-FAD adopts the function of an iron-sulfur cluster.

Author Contributions—N. P. C. and W. B. designed the study and wrote the manuscript. K. K. performed initial experiments. N. P. C. produced and purified recombinant flavodoxin and studied its reactions with Etf + Bcd and Rnf. A. S. performed the metal analysis. All authors analyzed the results and approved the final version of the manuscript.

Acknowledgments—We thank Professor Rudolf K. Thauer, Max-Planck-Institut für terrestrische Mikrobiologie, Marburg, for very helpful discussions and advice, and Professor Johann Heider, Philipps-Universität Marburg, for help with the modified Michaelis-Menten equation. We are indebted to Gabriela Mielke, Institut für Pharmazeutische Chemie, Philipps-Universität Marburg, for initial Na^+-determinations by flame photometry.

References

1. Louis, P., and Flint, H. J. (2009) Diversity, metabolism and microbial ecology of butyrate-producing bacteria from the human large intestine. *FEMS Microbiol. Lett.* **294,** 1–8
2. Chung, W. S., Walker, A. W., Louis, P., Parkhill, J., Vermeiren, J., Bosscher, D., Duncan, S. H., and Flint, H. J. (2016) Modulation of the human gut microbiota by dietary fibres occurs at the species level. *BMC Biol.* **14,** 3
3. Bienenstock, J., Kunze, W., and Forsythe, P. (2015) Microbiota and the gut-brain axis. *Nutr. Rev.* **73,** Suppl. 1, 28–31
4. Vital, M., Penton, C. R., Wang, Q., Young, V. B., Antonopoulos, D. A., Sogin, M. L., Morrison, H. G., Raffals, L., Chang, E. B., Huffnagle, G. B., Schmidt, T. M., Cole, J. R., and Tiedje, J. M. (2013) A gene-targeted approach to investigate the intestinal butyrate-producing bacterial community. *Microbiome* **1,** 8
5. Herrmann, G., Jayamani, E., Mai, G., and Buckel, W. (2008) Energy conservation via electron-transferring flavoprotein in anaerobic bacteria. *J. Bacteriol.* **190,** 784–791
6. Li, F., Hinderberger, J., Seedorf, H., Zhang, J., Buckel, W., and Thauer, R. K. (2008) Coupled ferredoxin and crotonyl coenzyme A (CoA) reduction with NADH catalyzed by the butyryl-CoA dehydrogenase/Etf complex from *Clostridium kluyveri*. *J. Bacteriol.* **190,** 843–850
7. Buckel, W., and Thauer, R. K. (2013) Energy conservation via electron bifurcating ferredoxin reduction and proton/Na^+ translocating ferredoxin oxidation. *Biochim. Biophys. Acta* **1827,** 94–113
8. Boiangiu, C. D., Jayamani, E., Brügel, D., Herrmann, G., Kim, J., Forzi, L., Hedderich, R., Vgenopoulou, I., Pierik, A. J., Steuber, J., and Buckel, W. (2005) Sodium ion pumps and hydrogen production in glutamate fermenting anaerobic bacteria. *J. Mol. Microbiol. Biotechnol.* **10,** 105–119
9. Biegel, E., and Müller, V. (2010) Bacterial Na^+-translocating ferredoxin: NAD^+ oxidoreductase. *Proc. Natl. Acad. Sci. U.S.A.* **107,** 18138–18142
10. Chowdhury, N. P., Mowafy, A. M., Demmer, J. K., Upadhyay, V., Koelzer, S., Jayamani, E., Kahnt, J., Hornung, M., Demmer, U., Ermler, U., and Buckel, W. (2014) Studies on the mechanism of electron bifurcation catalyzed by electron transferring flavoprotein (Etf) and Butyryl-CoA dehydrogenase (Bcd) of *Acidaminococcus fermentans*. *J. Biol. Chem.* **289,** 5145–5157
11. Chowdhury, N. P., Kahnt, J., and Buckel, W. (2015) Reduction of ferredoxin or oxygen by flavin-based electron bifurcation in *Megasphaera elsdenii*. *FEBS J.* **282,** 3149–3160
12. Campbell, C., Adeolu, M., and Gupta, R. S. (2015) Genome-based taxonomic framework for the class *Negativicutes*: division of the class *Negativicutes* into the orders *Selenomonadales emend., Acidaminococcales* ord. nov., and *Veillonellales* ord. nov. *Int. J. Syst. Evol. Microbiol.* **65,** 3203–3215
13. Mayhew, S. G., and Tollin, G. (1992) General properties of flavodoxins. in *Chemistry and Biochemistry of Flavoenzymes* (Müller, F., ed), pp. 389–426, CRC Press, Inc., Boca Raton
14. Thamer, W., Cirpus, I., Hans, M., Pierik, A. J., Selmer, T., Bill, E., Linder, D., and Buckel, W. (2003) A two [4Fe-4S]-cluster-containing ferredoxin as an alternative electron donor for 2-hydroxyglutaryl-CoA dehydratase from *Acidaminococcus fermentans*. *Arch. Microbiol.* **179,** 197–204
15. Hans, M., Bill, E., Cirpus, I., Pierik, A. J., Hetzel, M., Alber, D., and Buckel, W. (2002) Adenosine triphosphate-induced electron transfer in 2-hydroxyglutaryl-CoA dehydratase from *Acidaminococcus fermentans*. *Biochemistry* **41,** 5873–5882
16. Buckel, W. (1986) Biotin-dependent decarboxylases as bacterial sodium pumps: purification and reconstitution of glutaconyl-CoA decarboxylase from *Acidaminococcus fermentans*. *Methods Enzymol.* **125,** 547–558
17. Parthasarathy, A., Pierik, A. J., Kahnt, J., Zelder, O., and Buckel, W. (2011) Substrate specificity of 2-hydroxyglutaryl-CoA dehydratase from *Clostridium symbiosum*: toward a bio-based production of adipic acid. *Biochemistry* **50,** 3540–3550
18. Zehnder, A. J. B., and Wuhrmann, K. (1976) Titanium(III) citrate as a nontoxic oxidation-reduction buffering system for the culture of obligate anaerobes. *Science* **194,** 1165–1166
19. Chang, Y. J., Pukall, R., Saunders, E., Lapidus, A., Copeland, A., Nolan, M., Glavina Del Rio, T., Lucas, S., Chen, F., Tice, H., Cheng, J. F., Han, C., Detter, J. C., Bruce, D., Goodwin, L., *et al.* (2010) Complete genome sequence of *Acidaminococcus fermentans* type strain (VR4). *Stand. Genomic Sci.* **3,** 1–14
20. Brock, M., and Buckel, W. (2004) On the mechanism of action of the antifungal agent propionate. *Eur. J. Biochem.* **271,** 3227–3241
21. Nakos, G., and Mortenson, L. (1971) Purification and properties of hydrogenase, an iron sulfur protein, from *Clostridium pasteurianum* W5. *Biochim. Biophys. Acta* **227,** 576–583
22. Bradford, M. M. (1976) A rapid and sensitive method for the quantitation of microgram quantities of protein utilizing the principle of protein-dye binding. *Anal. Biochem.* **72,** 248–254
23. Laemmli, U. K. (1970) Cleavage of structural proteins during the assembly of the head of bacteriophage T4. *Nature* **227,** 680–685

24. Ziegenhorn, J., Senn, M., and Bücher, T. (1976) Molar absorptivities of β-NADH and β-NADPH. *Clin. Chem.* **22,** 151–160
25. Dawson, R. M. C., Elliott, D. C., Elliott, H. C., and Jones, K. M. (1986) *Data for Biochemical Research*, 3rd Ed., Clarendon Press, Oxford
26. Fillat, M. F., Borrias, W. E., and Weisbeek, P. J. (1991) Isolation and overexpression in *Escherichia coli* of the flavodoxin gene from *Anabaena* PCC 7119. *Biochem. J.* **280,** 187–191
27. Massey, V., and Palmer, G. (1966) On the existence of spectrally distinct classes of flavoprotein semiquinones: a new method for the quantitative production of flavoprotein semiquinones. *Biochemistry* **5,** 3181–3189
28. Sato, K., Nishina, Y., and Shiga, K. (2013) Interaction between NADH and electron-transferring flavoprotein from *Megasphaera elsdenii*. *J. Biochem.* **153,** 565–572
29. Chowdhury, N. P. (2014) *On the Mechanism of Electron Bifurcation by Electron Transferring Flavoprotein and Butyryl-CoA Dehydrogenase*. Ph.D. thesis, Philipps-Universität, Marburg, Germany
30. Jayamani, E. (2011) *A Unique Way of Energy Conservation in Glutamate Fermenting Clostridia*. Ph.D thesis, Philipps-Universität Marburg, Germany
31. Imkamp, F., Biegel, E., Jayamani, E., Buckel, W., and Müller, V. (2007) Dissection of the caffeate respiratory chain in the acetogen *Acetobacterium woodii*: identification of an Rnf-type NADH dehydrogenase as a potential coupling site. *J. Bacteriol.* **189,** 8145–8153
32. Hess, V., Schuchmann, K., and Müller, V. (2013) The ferredoxin:NAD^+ oxidoreductase (Rnf) from the acetogen *Acetobacterium woodii* requires Na^+ and is reversibly coupled to the membrane potential. *J. Biol. Chem.* **288,** 31496–31502
33. Steuber, J., Vohl, G., Casutt, M. S., Vorburger, T., Diederichs, K., and Fritz, G. (2014) Structure of the *V. cholerae* Na^+-pumping NADH:quinone oxidoreductase. *Nature* **516,** 62–67
34. Hess, V., González, J. M., Parthasarathy, A., Buckel, W., and Müller, V. (2013) Caffeate respiration in the acetogenic bacterium *Acetobacterium woodii*: a coenzyme A loop saves energy for caffeate activation. *Appl. Environ. Microbiol.* **79,** 1942–1947
35. Buckel, W., and Semmler, R. (1982) A biotin-dependent sodium pump: glutaconyl-CoA decarboxylase from *Acidaminococcus fermentans*. *FEBS Lett.* **148,** 35–38
36. Dimroth, P., and Thomer, A. (1986) Kinetic analysis of the reaction mechanism of oxaloacetate decarboxylase from *Klebsiella aerogenes*. *Eur. J. Biochem.* **156,** 157–162
37. Buckel, W., Zhang, J., Friedrich, P., Parthasarathy, A., Li, H., Djurdjevic, I., Dobbek, H., and Martins, B. M. (2012) Enzyme catalyzed radical dehydrations of hydroxy acids. *Biochim. Biophys. Acta* **1824,** 1278–1290
38. Buckel, W. (2001) Sodium ion-translocating decarboxylases. *Biochim. Biophys. Acta* **1505,** 15–27
39. Anderson, R. F. (1983) Energetics of the one-electron reduction steps of riboflavin, FMN and FAD to their fully reduced forms. *Biochim. Biophys. Acta* **722,** 158–162
40. Talfournier, F., Munro, A. W., Basran, J., Sutcliffe, M. J., Daff, S., Chapman, S. K., and Scrutton, N. S. (2001) αArg-237 in *Methylophilus methylotrophus* (sp. W3A1) electron-transferring flavoprotein affords ~200-millivolt stabilization of the FAD anionic semiquinone and a kinetic block on full reduction to the dihydroquinone. *J. Biol. Chem.* **276,** 20190–20196
41. Nitschke, W., and Russell, M. J. (2012) Redox bifurcations: mechanisms and importance to life now, and at its origin: a widespread means of energy conversion in biology unfolds. *Bioessays* **34,** 106–109
42. Toogood, H. S., van Thiel, A., Basran, J., Sutcliffe, M. J., Scrutton, N. S., and Leys, D. (2004) Extensive domain motion and electron transfer in the human electron transferring flavoprotein/medium chain acyl-CoA dehydrogenase complex. *J. Biol. Chem.* **279,** 32904–32912
43. Cornforth, J. W. (1959) Biosynthesis of fatty acids and cholesterol considered as chemical processes. *J. Lipid Res.* **1,** 3–28
44. Kim, J., Darley, D. J., Buckel, W., and Pierik, A. J. (2008) An allylic ketyl radical intermediate in clostridial amino-acid fermentation. *Nature* **452,** 239–242
45. Osyczka, A., Moser, C. C., and Dutton, P. L. (2005) Fixing the Q cycle. *Trends Biochem. Sci.* **30,** 176–182
46. Sazanov, L. A., and Hinchliffe, P. (2006) Structure of the hydrophilic domain of respiratory complex I from *Thermus thermophilus*. *Science* **311,** 1430–1436
47. Bertsch, J., Parthasarathy, A., Buckel, W., and Müller, V. (2013) An electron-bifurcating caffeyl-CoA reductase. *J. Biol. Chem.* **288,** 11304–11311
48. Weghoff, M. C., Bertsch, J., and Müller, V. (2015) A novel mode of lactate metabolism in strictly anaerobic bacteria. *Environ. Microbiol.* **17,** 670–677
49. Kaster, A. K., Moll, J., Parey, K., and Thauer, R. K. (2011) Coupling of ferredoxin and heterodisulfide reduction via electron bifurcation in hydrogenotrophic methanogenic archaea. *Proc. Natl. Acad. Sci. U.S.A.* **108,** 2981–2986
50. Wang, S., Huang, H., Moll, J., and Thauer, R. K. (2010) $NADP^+$ reduction with reduced ferredoxin and $NADP^+$ reduction with NADH are coupled via an electron-bifurcating enzyme complex in *Clostridium kluyveri*. *J. Bacteriol.* **192,** 5115–5123
51. Wang, S., Huang, H., Kahnt, J., and Thauer, R. K. (2013) A reversible electron-bifurcating ferredoxin- and NAD-dependent [FeFe]-hydrogenase (HydABC) in *Moorella thermoacetica*. *J. Bacteriol.* **195,** 1267–1275
52. Wang, S., Huang, H., Kahnt, J., and Thauer, R. K. (2013) *Clostridium acidurici* electron-bifurcating formate dehydrogenase. *Appl. Environ. Microbiol.* **79,** 6176–6179
53. Schuchmann, K., and Müller, V. (2012) A bacterial electron-bifurcating hydrogenase. *J. Biol. Chem.* **287,** 31165–31171
54. Schut, G. J., and Adams, M. W. (2009) The iron-hydrogenase of *Thermotoga maritima* utilizes ferredoxin and NADH synergistically: a new perspective on anaerobic hydrogen production. *J. Bacteriol.* **191,** 4451–4457
55. Mitchell, P. (1976) Possible molecular mechanisms of the protonmotive function of cytochrome systems. *J. Theor. Biol.* **62,** 327–367

Reduction of Flavodoxin by Electron Bifurcation and Sodium Ion-dependent Reoxidation by NAD$^+$ Catalyzed by Ferredoxin-NAD$^+$ Reductase (Rnf)

Nilanjan Pal Chowdhury, Katharina Klomann, Andreas Seubert and Wolfgang Buckel

J. Biol. Chem. 2016, 291:11993-12002.
doi: 10.1074/jbc.M116.726299 originally published online April 5, 2016